Supplementary information

Improved broadband and omnidirectional light absorption in silicon nanopillars achieved through gradient mesoporosity induced leaky waveguide modulation

Prajith Karadan[a,b], Aji. A. Anappara[b], V. H. S. Moorthy[c], Chandrabhas Narayana[d], and Harish C. Barshilia*[a]

The RMS surface roughness values of the SiNPLs etched for different time durations are shown in Fig. S1. The surface roughness of SiNPLs etched 2, 5, 7 and 10 min are 152, 329, 546 and 932 nm, respectively.

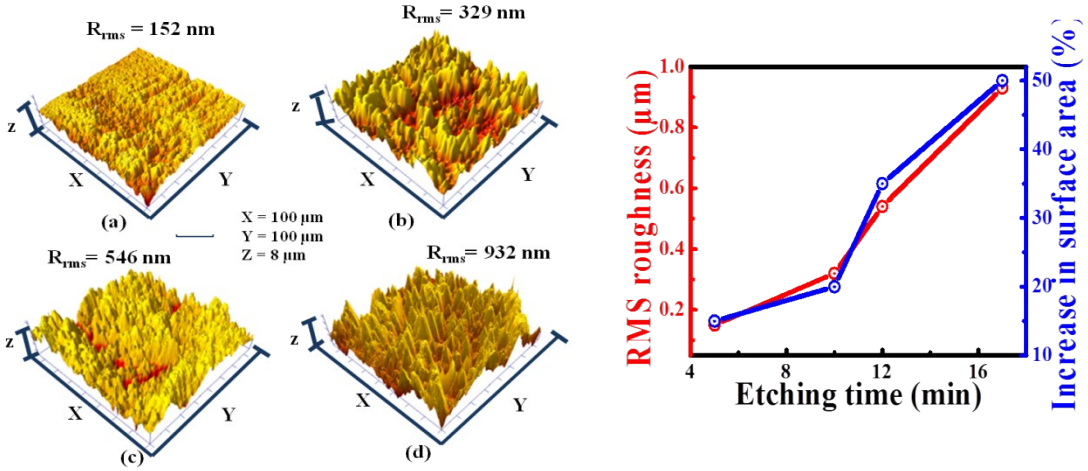

Fig. S1 (a) RMS roughness of SiNPLs etched for different time durations. (b) Variation of RMS roughness and increase in surface area with etching time.

The simulated and experimental reflectance spectra of bare Si and SiNPLs are compared in Fig. S1. As we have already seen in the manuscript, the simulated and experimental reflectance spectra of bare Si shows a reflectance >30% in the visible region, shown in Fig. S1(a). The simulated electric field distribution of bare Si is shown in Fig S2(b). The surface of bare Si is optically smooth for the incident light, hence the electric field distribution is found to be same everywhere.

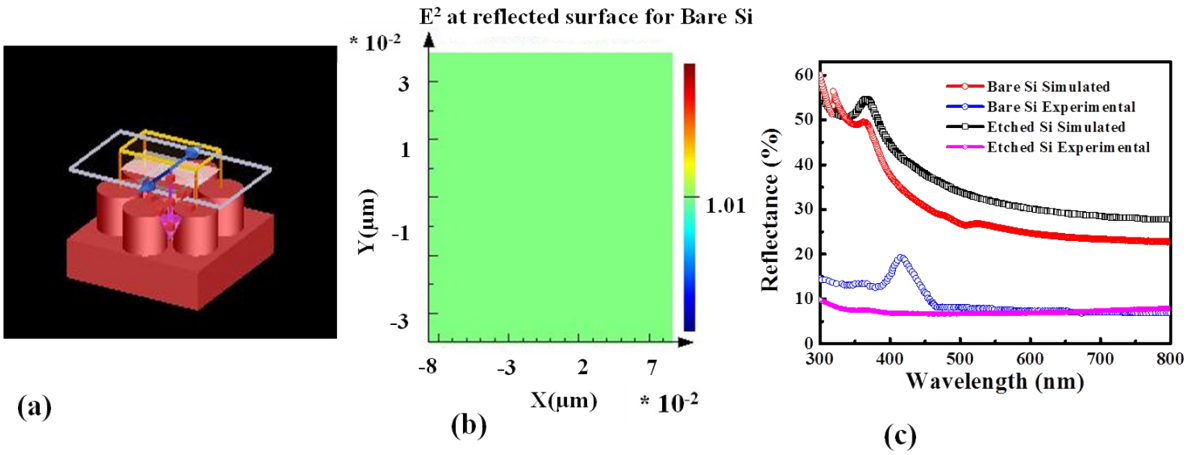

Fig. S2 (a) The model used for simulation. (b) Simulated and experimental reflectance of bare Si and SiNPLs. (c) Simulated electric field plot for bare Si

We have simulated the TE and TM waveguide mode associated with the SiNPLs, shown in Fig. 4 in the main manuscript. TE mode means the waveguide mode generated using TE plane wave (90º polarization) as the source in the Simulation. TM modes are the waveguide mode associated with SiNPLs using TM plane wave (0º polarization) as the source. For TE polarized light magnetic field component $H=H_z$ and electric field component $E_z = 0$. For TM polarized light $E=E_z$ and $H_z =0$.

The FWHM variation of the crystalline as well as the peak arises from the porosity is plotted as a function of angle of incidence, shown in Fig. S3(a). The low frequency Raman peak at 300 cm^{-1} represents the second order acoustic (2TA) modes. The intensity of 2TA peak is found to be increased with angle of incidence varying from 0-45, shown in Fig. S3(b).

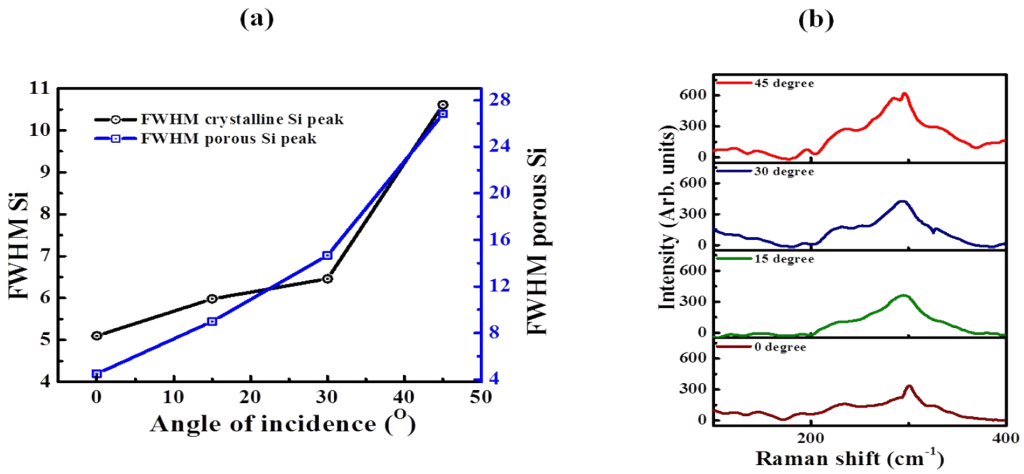

Fig. S3. (a) Variation of FWHM of crystalline Si peak and porous Si peak with angle of incidence in the Raman spectra of SiNPLs. (b) Low frequency acoustic phonon modes (2TA) observed in angle dependent Raman spectra of SiNPLs.

The schematic representation of mesoporous SiNPLs with gradient porosity is shown in Fig. S4 (a). Fig. S4 (b) shows the FDTD model for the simulation of SiNPLs with step discontinuity. This model shows close resemblance with the gradient refractive index condition. The simulated results along with the experimental reflectance are plotted in Fig. S4 (c). The exeperimental reflectance of the SiNPLs is in good agreement with the simulated SiNPLs with step discontinuity over the entire wavelength. So, we confirmed the reflectance mismatch at the lower wavelength region in Fig. 3(d) is due to the gradient refractive index condition, which arises from the inhomogeneous mesoporous structures on the SiNPLs.

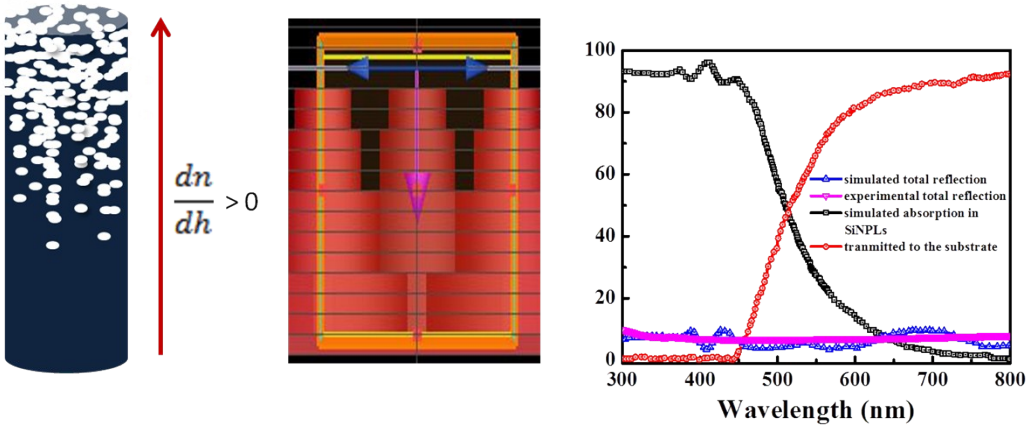

Fig. S4. (a)The schematic to show the graded porosity (b) FDTD model for simulation of SiNPLs with step discontinuity (c) simulated results with the experimental reflectance data.

The SiNPLs with hcp close packed structure is equivalent to a two dimensional photonic crystal, which has periodicity along X, Y directions and inhomogeneous along Z direction. We simulated the band structure of SiNPLs by keeping the refractive index contrast between air and SiNPLs 2.9, 2.4 respectively, shown in Fig. given below. Simulated band structure shows good agreement with the literature[1].

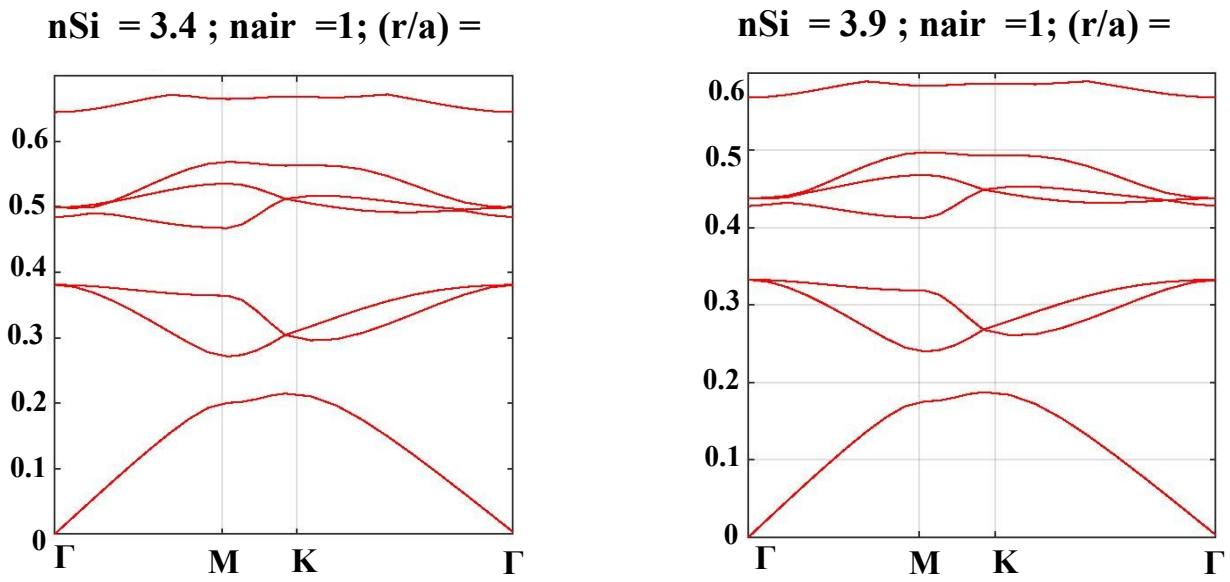

Fig. S5. Simulated band structure of periodic array of SiNPLs